atmosphere

MDPI

Article

Temporal Profiles of Volatile Organic Compounds near the Houston Ship Channel, Texas

Meghan Guagenti [1], Sujan Shrestha [1,†], Manisha Mehra [1,‡], Subin Yoon [2], Mackenzie T. S. Ramirez [3], James H. Flynn III [2] and Sascha Usenko [1,3,*]

[1] Department of Environmental Science, Baylor University, Waco, TX 76076, USA
[2] Department of Earth and Atmospheric Sciences, University of Houston, Houston, TX 77204, USA; jhflynn@central.uh.edu (J.H.F.III)
[3] Department of Chemistry and Biochemistry, Baylor University, Waco, TX 76706, USA
* Correspondence: sascha_usenko@baylor.edu
† Current address: Department of Atmospheric Sciences, Rosenstiel School of Marine, Atmospheric and Earth Science, University of Miami, Miami, FL 33149, USA.
‡ Current address: Department of Chemical, Environmental, and Materials Engineering, University of Miami, Miami, FL 33149, USA.

Abstract: Houston, Texas, with its large-scale industrial activities, serves as a national hub for petrochemical processing and chemical feedstock production, making it a unique emission region for volatile organic compounds (VOCs) and production-related emissions. These emissions can be associated with industrial activities, including solvent usage and production to manufacture consumer products such as volatile chemical products. To support the Houston-based Dept. of Energy's Atmospheric Measurement Radiation program-led Tracking Aerosol Convection ExpeRiment (TRACER) projects, VOCs were measured at the San Jacinto Battleground State Historic Site during September 2021 and 2022. The observed VOC mixing ratios reveal unique emission signatures for select VOCs, including benzene, toluene, acetone, and isoprene. Routine nighttime enhancements of these compounds exceeded the urban background, with mixing ratios increasing by up to 20 ppbv per hour and persisting for up to 6 h, suggesting that emissions from local industrial activities near the Houston Ship Channel (HSC) are impacting the site. For example, mixing ratios exceeding 15 ppbv for at least one VOC were observed on 58% of nights (n = 32 nights), with 19 nights (~35%) having two or more VOCs with mixing ratios above 15 ppbv. For select peak emission events, the NOAA dispersion model estimated plume transport across parts of the urban system, suggesting that VOCs from the HSC may impact local air quality. This study highlights the importance of VOC-related emissions from industrial production and supply chains in contributing to total VOC emissions in urban areas like Houston, Texas.

Keywords: benzene; acetone; isoprene; PTR-MS; petrochemical; chemical feedstocks

check for updates

Academic Editor: Jinian Shu

Received: 18 December 2024
Revised: 31 January 2025
Accepted: 18 February 2025
Published: 24 February 2025

Citation: Guagenti, M.; Shrestha, S.; Mehra, M.; Yoon, S.; Ramirez, M.T.S.; Flynn, J.H., III; Usenko, S. Temporal Profiles of Volatile Organic Compounds near the Houston Ship Channel, Texas. *Atmosphere* **2025**, *16*, 260. https://doi.org/10.3390/atmos16030260

Copyright: © 2025 by the authors. Licensee MDPI, Basel, Switzerland. This article is an open access article distributed under the terms and conditions of the Creative Commons Attribution (CC BY) license (https://creativecommons.org/licenses/by/4.0/).

1. Introduction

Volatile organic compounds (VOCs) play a crucial role in tropospheric chemistry as they can serve as precursors for secondary organic aerosol (SOA) and ozone (O_3) formation [1,2]. VOCs can be emitted into an urban airshed from a variety of biogenic and anthropogenic sources, including local green spaces, motor vehicle exhaust, industrial activities, solvent usage, and consumer products. Historically, motor vehicle emissions represented a substantial fraction of urban emission inventories [3]. However, advancements in vehicle emission controls and the transition towards fleet electrification have

shifted the urban VOC emission profile towards nonmobile sources, including emissions from a subset of VOCs known as volatile chemical products (VCPs), which can account for more than 50% of urban VOC emissions [4]. VCPs are often petrochemically derived, as the petrochemical industry has expanded its activities beyond oil and gas processing to include a wide range of consumer products, such as plastics, cleaners, industrial solvents, adhesives, and pesticides [5–8]. As a result, emissions from the petrochemical industry may impact local air quality by acting as a source of both VOCs and VCPs, depending on the activity or product being produced. These changes in emissions may result in a more diverse chemical profile and varying temporal and spatial emission patterns, which could potentially impact atmospheric processing and the total urban VOC composition. It is important to note that VOC and VCP emissions may change with fluctuations in industrial activity and technology and shifts in product output. Furthermore, industrial operations may be influenced by feedstock availability, shared infrastructure, and broader global economic activities [9].

Houston, Texas, is situated at a land–sea interface and has the second fastest-growing metropolitan population in the United States [10]. The proximity to the Gulf of Mexico has enabled the development of the Houston Ship Channel (HSC) as a national hub for the petrochemical industry, which can contribute to local air quality conditions. The HSC hosts a wide range of complex and diverse emission sources from the petrochemical supply chain, including oil refineries, chemical feedstocks, chemical transportation, and chemical transfer stations. Over the last two decades, a series of multi-institution Houston-based field campaigns have been aimed at better understanding the sources, including the HSC, and atmospheric processes driving the formation and distribution of secondary products [11–18]. Based on its unique urban and industrial emission sources and meteorological conditions, Houston and the HSC were selected to host the Dept. of Energy's Atmospheric Measurement Radiation program-led Tracking Aerosol Convection ExpeRiment (TRACER) project (https://www.arm.gov/research/campaigns/amf2021tracer, last access date: 19 September 2024). The TRACER project was accompanied by several TRACER-related projects, including NASA TRACER-Air Quality (TRACER-AQ; https://www-air.larc.nasa.gov/missions/tracer-aq/index.html, last access date: 19 September 2024) and the Texas Commission on Environmental Quality (TCEQ) TRACER-AQ1 and -AQ2 (2021 and 2022, respectively). VOC emissions at petrochemical processing sites, such as the HSC, can be highly variable depending on different industrial activities. For example, factors such as the chemical loading process (e.g., top-loading vs. bottom-loading), loading temperature and pressure, the usage and condition of the vapor recovery system during chemical storage and transfer, and changes in the frequency of emergency venting or flaring at the facility, can contribute to fluctuations in VOC emissions. As a result, there is a knowledge gap in urban VOC emission characterization near the petrochemical supply chain, including industrial refinement and processing of VCPs. In addition, these processing sites may also use chemical feedstocks of compounds typically associated with biogenic sources, such as isoprene, in VCP production. This shift in VOC sources from biogenic to industrial sources can alter the spatial and temporal distributions of these compounds, thereby influencing their atmospheric processing and formation of secondary products. Assessing the temporal variability of petrochemical processing emissions and their impacts on air quality is particularly important for areas near petrochemical and manufacturing hubs. To examine VOC emissions from industrial sources in and around the HSC, yearly averages of speciated VOCs are self-reported by facilities to provide information on emission magnitude and type (e.g., stack, flare, and fugitive sources) to the public (https://www.tceq.texas.gov/airquality/point-source-ei, last access date: 20 February 2025). However, the annual data do not provide the temporal resolu-

tion needed to characterize the primary VOC emissions from various industrial emission sources or activities, making it difficult to provide guidance for effective mitigation efforts. This issue is further compounded when considering secondary pollution formation, as plume mixing can be rapid and highly time-dependent, making it difficult to assess using annual datasets.

In support of the TRACER project goals, the aim of this work was to examine the VOCs from petrochemical processing in and around the HSC as an important contributor to ambient concentrations. To this end, VOC mixing ratios were measured using a proton-transfer-reaction mass spectrometer at a site adjacent to the HSC during September 2021 and 2022. Using the real-time VOC observations, we aimed to (1) characterize VOC mixing ratios and assess their variability near the HSC, (2) quantify the diurnal variability in select VOCs across September 2021 and 2022 measurement campaigns, and, finally, (3) assess VOC plume transport capabilities from the Battleground site to surrounding communities. These results are relevant to the communities within our study domain, as well as improving atmospheric models and human health risk assessments of these facility areas.

2. Materials and Methods

The presented measurements were collected as part of TRACER-AQ1 (2021) and TRACER-AQ2 (2022). Shrestha et al. [19] previously described the sampling site, mobile laboratory, and VOC instrumentation utilized during the TRACER campaigns and presented the 2021 VOC data included in this study. The current study built on the 2021 dataset by including the 2022 VOC observations, which enabled the annual variability to be assessed here. A description of the sampling setup and measurements has also been included in the Supplementary Materials (Figure S1). The ARM Data Discovery portal provides access to the real-time VOC measurements, including the benzene, acetone, and isoprene species discussed below, and the wind data presented in this work (https://adc.arm.gov/discovery/#/, last access date: 9 July 2024). The Houston-based Point Source Emission Inventory can be accessed through the TCEQ (https://www.tceq.texas.gov/airquality/point-source-ei, last access date: 9 July 2024).

2.1. Houston Ship Channel Sampling

The Baylor University and University of Houston-operated Mobile Air Quality Laboratory (MAQL2) was deployed to the San Jacinto Battleground State Historic Site (29.752° N, 95.091° W), located along the Houston Ship Channel, from 1 to 30 September 2021 and from 5 to 30 September 2022. The Battleground site is located within an industrial area surrounded by petroleum storage and manufacturing facilities, as well as shipping and rail terminals and pipeline services supporting petrochemical transportation, enabling near-facility source measurements. According to the self-reported point source emission inventory, there are over 880 benzene, 210 acetone, and 50 isoprene sources within 8 km of the sampling site (see Figures S2–S4). Downwind transport from outside the local industrial area, including nearby fence-line communities, may also influence the site based on the observed wind direction and speed. Additionally, the site is near several highways: Interstate Highway 10 to the north, Texas State Highway 8 to the west, and Texas State Highway 225 to the south.

2.2. Mobile Air Quality Laboratory (MAQL2)

During both TRACER campaigns, the instrumentation was housed in the MAQL2, which is a 35 m^3 insulated, air-conditioned trailer with an ~10 m telescoping tower and inlet box that extends above the trailer during stationary measurements. Wind direction and speed measurements were also collected on the tower. Real-time VOC measurements

were collected using a heated sampling line set at 70 °C (Atmo-Seal Engineering Inc., Troy, MI, USA) and averaged to five minutes to match the meteorological datasets.

2.3. Instrumentation

VOCs were measured using a quadrupole proton-transfer-reaction mass spectrometer during both TRACER campaigns (PTR-QMS-300; Ionicon Analytik, Innsbruck, Austria). Details on the PTR-MS operation, calibration, and data processing used here are presented in our previous publications [19,20]. Briefly, ambient air is drawn through a perfluoroalkoxy (PFA) Teflon-lined manifold at a rate of 8 lpm, from which a subsample of 100 sccm is drawn to the PTR-MS. A sample drying system similar to that used by Jobson and McCoskey (2010) was implemented to reduce any effects of water vapor that can occur while operating the drift tube of the PTR-MS at a lower E/N ratio (i.e., 100 Td) [21]. The sampled gas molecules undergo chemical ionization via proton transfer from protonated water (H_3O^+) in the drift tube and are then directed to the quadrupole mass spectrometer for quantification. While the PTR-MS can operate in other ionization modes, the analytes included in this study were measured in the H_3O^+ mode, and a table of the ions used for each analyte can be found in the Supplementary Materials (Table S1). For more information on the potential interferences from other VOC fragments in the PTR-MS measurements, please refer to the Supplementary Materials.

Single-point calibrations and zeros were run daily, and multi-point calibrations were performed at the start and end and periodically throughout the campaign (see SI). The dynamic linear range (DLR) of the PTR-MS measurements spanned from approximately 3 ppbv to 40 ppbv, with values outside of this range considered tentative assignments (Table S2). The PTR-MS measurements reported here were obtained using the daily calibration of individual mass against the known concentration of the calibration mixture of VOCs. Zero air was generated by passing laboratory air through a heated catalyst (alumina on palladium at 350 °C). VOC data were collected with approximately 30 s time scans and were averaged to longer time scales, typically 5 min, to match the final averaged data from other instruments deployed during the campaign.

2.4. Data Analysis

2.4.1. Enhancement Period Identification

VOC plumes were identified as periods with values exceeding the monthly average and one standard deviation ($\mu + \sigma$) for longer than five minutes to distinguish between periods larger than the background. This approach has been used previously to identify plumes from time-series data [22,23].

2.4.2. NOAA HYSPLIT Dispersion Model

The NOAA Hybrid Single-Particle Lagrangian Integrated Trajectory (HYSPLIT) Dispersion Model estimates the forward transport of air parcels emitted from a given location based on ambient meteorological parameters. In this study, select periods of the two campaigns were chosen to visualize the VOC transport across the Houston Metropolitan Area by modeling emissions from the Battleground site. The model inputs are noted in the Supplementary Materials (Figure S5), and potential limitations in interpreting the plume transport are discussed in Section 3.2.

3. Results and Discussion

3.1. VOC Mixing Ratios and Temporal Trends

At Battleground, the MAQL2 measured select VOC mixing ratios during September 2021 and 2022, including compounds emitted from biogenic and anthropogenic sources.

The measured VOC species included aromatics, such as benzene, toluene, and C_8 isomers (e.g., ethylbenzene and xylenes), as well as alkenes, like isoprene, and oxygenated VOCs, including acetone. These compounds are typically associated with industrial emissions, traffic sources, biogenic releases (e.g., stress responses of plants), and secondary formation processes. The VOC mixing ratios ranged from below the method detection limit to 200 ppbv, with all species routinely exceeding 10 ppbv across both measurement campaigns, indicating both urban background and periods of enhancements (Figures 1–3, S6 and S7). Note: VOC mixing ratios exceeding 40 ppbv are considered tentative assignments as they are beyond the DLR of the calibration curve used in this study (Table S2). Of the measured compounds, acetone consistently exhibited the largest mixing ratios, frequently surpassing 50 ppbv in September 2021 and 2022. Interestingly, isoprene mixing ratios over 100 ppbv were observed in 2021 [19], which were ten times higher than the maximum observed in 2022 (i.e., 10 ppbv). Among the aromatic species, benzene and C_8 isomers were routinely observed above urban background levels in both years, whereas toluene and styrene showed specific periods of enhancement, occurring at different times of the month during both years (e.g., toluene at the beginning and styrene in the second half of the month). Due to their elevated concentrations and multiple emission sources across the study area, benzene, toluene, C_8 isomers, acetone, and isoprene were selected for further discussion (Sections 3.2–3.4).

In both years, rapid enhancements in VOC mixing ratios were repeatedly observed for all measured species, particularly at night (Figures 1 and S6). Furthermore, these periods of enhancement typically increased between 5- and 10-fold over relatively short periods (1 to 5 h). For example, on 24 September 2022, acetone mixing ratios increased from 6 ppbv to >100 ppbv within an hour as part of an eight-hour enhancement period. Additionally, a sharp peak in benzene mixing ratios from 2 to 34 ppbv within an hour was also observed on 24 September 2022, and an estimated plume transport pathway across Harris County is described below (Figure 1; see Figure 4 in Section 3.2). Similarly, toluene, C_8 isomers, and acetone showed sharp nighttime enhancement peaks in both years. Altogether, the timing, magnitude, and rate of changes measured during these periods of enhanced VOC mixing ratios suggest the presence of strong local nighttime sources and help rule out traditional daytime VOC sources, such as solar-radiation-stress-induced biogenic emissions (e.g., isoprene) and motor vehicle emissions associated with rush-hour traffic (see the section below and Figures 1d–f, 2, and 5).

The impact of potential source wind sectors can be assessed by examining VOC concentrations as a function of wind direction (Figures 2 and S8). In this study, omnidirectional contributions were observed for all species during both measurement campaigns. Concentrations above the dashed lines in Figure 2 represent values above the monthly average (μ) + standard deviation (σ) to help distinguish between differences in urban background and VOC mixing ratio enhancements. In 2021, the observed benzene mixing ratios greater than $\mu + \sigma$ (i.e., >11 ppbv; maximum of ~60 ppbv) were associated with a southerly wind direction (135° to 225°). A similar pattern was observed in 2022; however, the peak mixing ratios from this sector (135° to 225°) were approximately half of the 2021 observations (i.e., >5 ppbv; maximum of ~35 ppbv). Within this sector, there are more than 40 self-reported independent benzene sources across multiple facilities, including flare, fugitive, and stack emission sources, all within ~4 km of the Battleground site (Figure S2). Top annual benzene emitters (~2 to 7 tons per year) include activities associated with equipment leaks, VOC processes, and wastewater handling. Acetone mixing ratio wind direction plots highlight bimodal peaks within the 180° to 295° sector, which may indicate contributions from southwestern sources and from the nearly 15 self-reported fugitive sources directly northwest across the Ship Channel (Figure S3). Interestingly, isoprene wind direction plots for 2021

and 2022 highlight the complexity of assessing VOCs that can be associated with biogenic and industrial sources. In 2021, the isoprene observations were an order of magnitude larger than the 2022 isoprene mixing ratios and had contributions primarily from the 90° to 135° and 190° to 225° sectors, which aligns with reported sources (Figures 2c,f and S8), with top annual emitters (~1 to 4 tons per year) including activities associated with storage tanks, loading, and equipment leaks. In contrast, the isoprene mixing ratios observed in 2022 were observed omnidirectionally and had daytime peaks with mixing ratios similar to the typical biogenic profile (Figures 2 and 6).

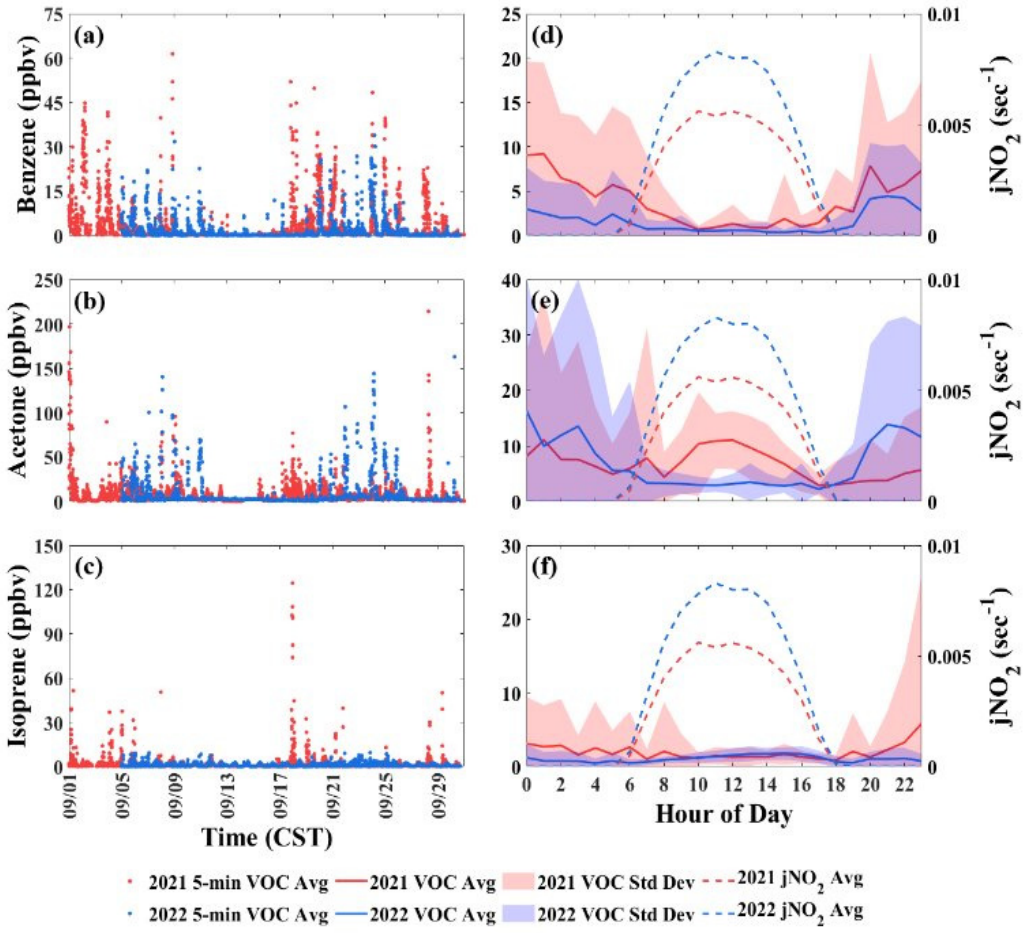

Figure 1. Time-series (**a**–**c**) and diurnal (**d**–**f**) mean profiles (μ + σ) of benzene, acetone, and isoprene measured in September 2021 (red traces) and September 2022 (blue traces) in the HSC. The 2022 diel mean of isoprene has been scaled to match 2021's measurements for ease of comparison. A properly scaled version of the isoprene figure (**f**) is provided in Section 3.4 (Figure 6). The average solar radiation (jNO_2) measured for September 2021 and 2022 is indicated with dashed lines. September 2021 measurements occurred from /1 September to 30 September, while September 2022 measurements occurred from 5 September to 30 September.

3.2. Benzene, Toluene, and C_8 Isomers

Benzene, toluene, and xylene (included in the C_8 isomers) are EPA-designated hazardous air pollutants (HAPs) and are often measured in plumes associated with anthropogenic sources (e.g., traffic emissions, industrial processes, gasoline storage and handling, and power or heat generation), with mixing ratios typically ranging from 0.2 to 2.5 ppbv in various cities [20,24,25]. Within a large petrochemical complex such as the HSC, these VOCs could also be associated with oil and natural gas activities, which can include oil refinement and distillation and petrochemical manufacturing [26]. In addition, the HSC also supports a wide range of chemical processing (i.e., feedstock production, storage,

and loading activities), which can also contribute to the emission of benzene, toluene, and C_8 isomers. For example, benzene can be used as a chemical feedstock to form key intermediate species during VCP production, including styrene, cumene, cyclohexane, and aniline [27–31]. With the ongoing decrease in vehicular emission contributions to urban emission inventories, the industrial-sources fraction may continue to grow, especially as the demand for base petrochemical feedstocks is predicted to grow in response to increasing demand for consumer products.

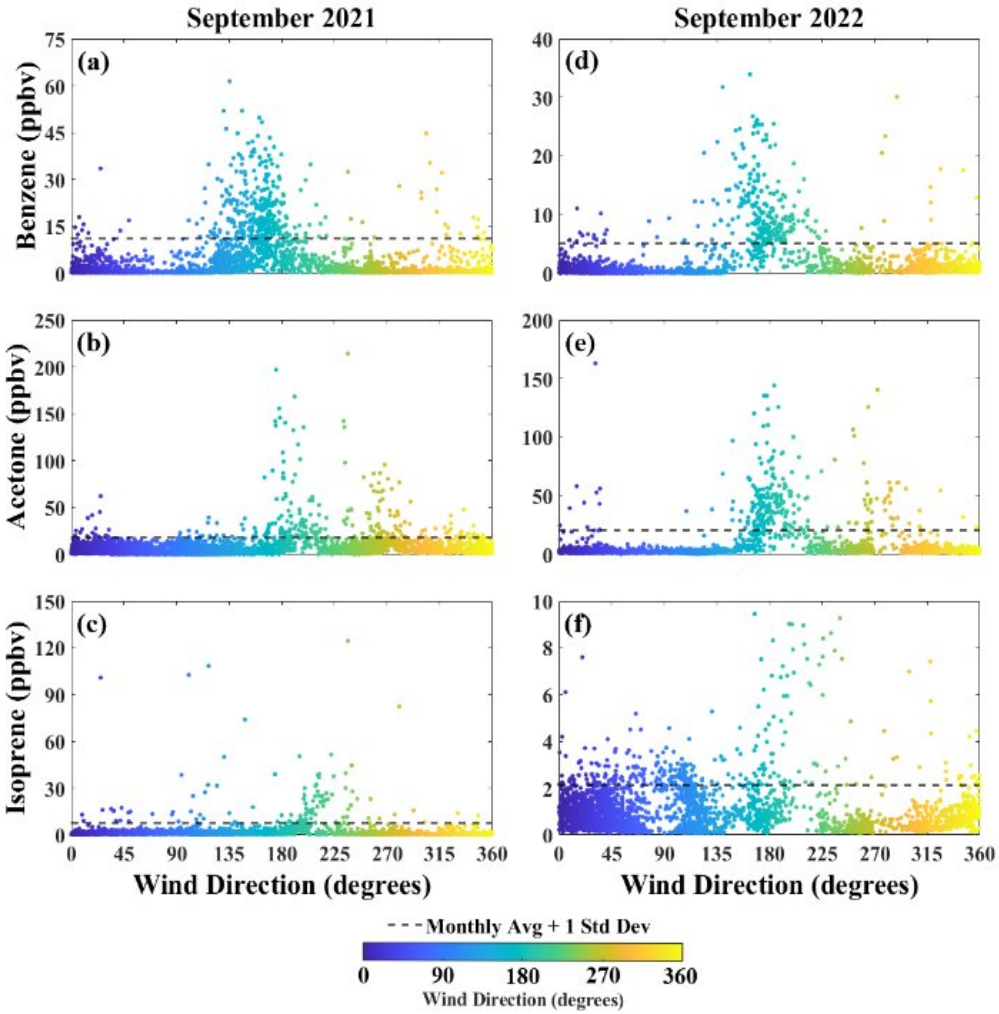

Figure 2. Wind direction vs. VOC concentrations for benzene, acetone, and isoprene in September 2021 (**a**–**c**) and 2022 (**d**–**f**). Wind direction is presented in degrees and color-coded. For example, wind arriving from the south (i.e., 180°) is represented by a teal green color. The horizontal dashed line represents the μ + σ threshold value for each compound during the two measurement campaigns.

Peaks of these HAPs primarily occurred at night; however, daytime peaks over 10 ppbv were also observed. For example, intermittent daytime and nighttime peaks in benzene mixing ratios (i.e., mixing ratios larger than μ + σ for five minutes) often exceeded 25 ppbv, with peaks ranging in durations from one to five hours. In September 2021 and 2022, benzene mixing ratios exceeding 25 ppbv were observed on 17 and 5 unique days, respectively, with all of these exceedances occurring during the period of 20:00–7:00. Currently, the TCEQ hourly averaged guideline for benzene exposure is 180 ppbv, which was raised from 25 ppbv in 2008. Reported VOC mixing ratios in November 2021 and 2022 measurements in communities downwind of the HSC (2–550 ppbv) were similar to observations made in this study [32]. As reported here, these nighttime pulse events highlight the magnitude and

possibly chronic nature of potential exposure to the surrounding communities. In addition, toluene peaks larger than 5 ppbv were also observed across both measurement campaigns, ranging from one to three hours. Due to the intermittent nature of the mixing ratio profiles, campaign averages of these VOC mixing ratios were not calculated. The sharp increases in benzene, toluene, and C_8 mixing ratios may suggest local sources with direct emissions that rapidly increase levels over a short period of time (h), followed by a sharp decline, which may highlight the immediate end of the activity and dispersion of the pollutants. In the HSC, there are various types of local benzene emitters, including fugitive emissions, stack releases, and flare sources. These emissions can arise from activities such as venting during the transfer of solvents from storage tanks to transport tanks for land or marine operations, emissions from blending or mixing tanks, and processes such as tank cleaning. According to the TCEQ point source emission inventory for Harris County, there are over 880 benzene and 920 toluene sources within an 8 km radius of the Battleground sampling site, with potential combined emissions exceeding 100 and 160 tons per year, respectively (Figure S2).

To examine potential nighttime benzene emission sources, a benzene-to-toluene ratio (B/T) was calculated using mixing ratios (Figure 3) and compared to known sources. As benzene and toluene are co-emitted during fossil fuel combustion, the B/T ratio in areas heavily impacted by vehicular emissions typically ranges from approximately 0.45 to 1.1 [33,34], and changes in the B/T ratio would suggest changes in benzene and toluene emission sources. High B/T ratios (e.g., >5) suggest that benzene is emitted as a single VOC (i.e., not with toluene), which helps eliminate sources that emit both benzene and toluene simultaneously, such as fossil fuel combustion. Similarly, high mixing ratios of toluene without significant benzene mixing ratios (see Figures 3 and S6) suggest that combustion sources are not the major source of toluene emissions at that time. The relationship between benzene and toluene mixing ratios was examined using a linear regression model. For the measurement periods, this statistical analysis yielded no or very weak correlations between mixing ratios of benzene and toluene ($r^2 < 0.1$; Tables S3 and S4). This lack of relationship between known co-emitted VOCs was not surprising, as the majority of peak benzene and toluene mixing ratios did not overlap temporally, which indicates independent sources of benzene and toluene. Similarly, benzene and toluene mixing ratios showed no or very weak correlations with C_8 isomers, which again suggests that these compounds are not co-emitted. The lack of co-emission suggests sources not associated with burning fossil fuels or petrochemical activities that involve mixtures of these compounds (e.g., fuel distillation). The magnitude of the mixing ratios, emission profiles, and temporal variability suggests sources that typically handle VOCs individually (such as storage, transfer, feedstock, and intermediate production), which match known TCEQ emission activities associated with the HSC's largest emitters. The magnitude of the sporadic events (Figure 1a), along with temporal differences (i.e., nighttime peaks; Figure 2d), wind direct data (Figure 2a), and weak correlations (Figure 3), suggest that emissions from local industrial activities likely contributed more to the ambient measurements than burning fossil fuels (e.g., local traffic emissions). Furthermore, this suggests that a portion of the benzene and toluene measured at Battleground may be related to activities associated with the production or usage of VCPs.

Identifying a single source in a dynamic system like the HSC industrial complex is extremely challenging. This is partly due to the high density of sources in close proximity, with hundreds of known emission sources within an 8 km radius (Figures S2–S4). The variability in activities associated with each source, along with the diversity of source types (e.g., equipment leaks), further complicates pinpointing specific emissions. For example, the frequency of filling and dispersing VOCs from storage tanks can vary based

on chemical usage at a given time. As chemical production fluctuates across various facilities, emissions throughout the industrial complex also change. These observations suggest that the measurements at the sampling site, or even over the entire month, represent the emissions of the industrial complex as a whole rather than any single facility of specific activity (e.g., solvent use, coatings, or painting). These results underscore that emissions are the result of a combination of multiple facilities and activities, all of which vary over time, across the day and night, from month to month and year to year. In fact, the density, proximity, and variability of facility operations make it exceptionally difficult to identify or characterize relatively strong point sources.

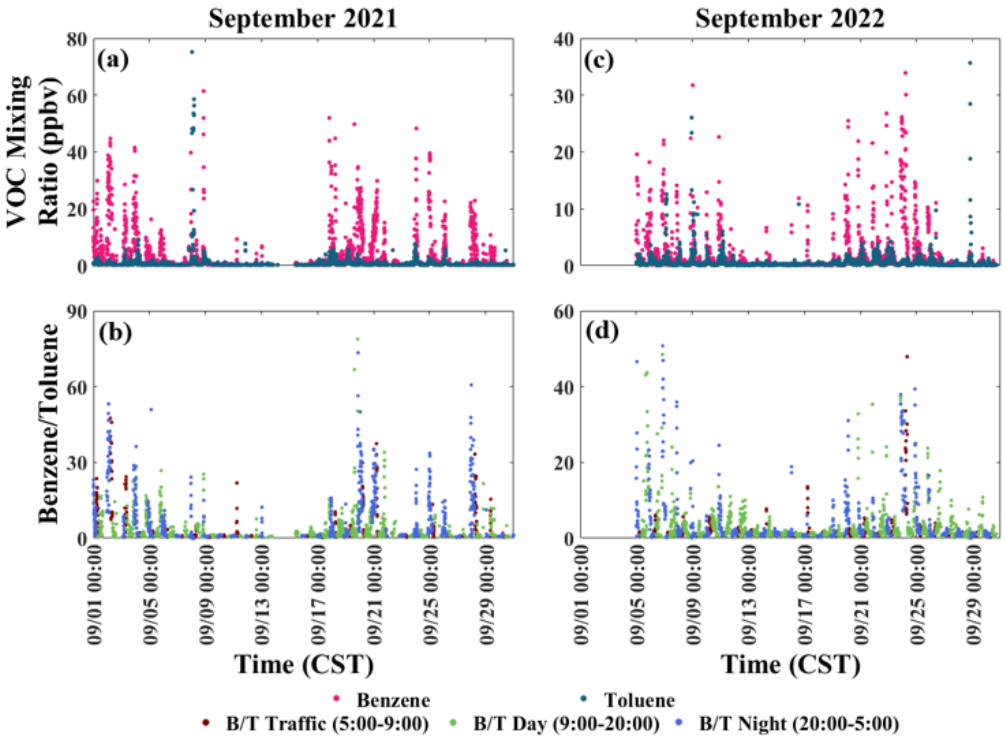

Figure 3. Benzene (**a**) and toluene (**c**) mixing ratios (ppbv) and benzene-to-toluene (B/T) ratios (**b**,**d**) for September 2021 and 2022 field campaigns. B/T ratios for specific periods of the day are differentiated by color (**b**,**d**). Mixing ratios exceeding approximately 40 ppbv are tentative assignments, as the mixing ratios were beyond the DLR of the calibration curve for the study.

After air masses arrive at the monitoring site, dispersion models can be used to estimate the air parcel's outward flow (Figures 4 and S9). For example, on the night of 23–24 September 2022, the MAQL2 captured the largest benzene mixing ratios of the month (>30 ppbv) as part of an enhanced period lasting from 20:30 to 06:30. The event's average mixing ratio (16 ppbv) was more than five times larger than the monthly nighttime average (3 ppbv) and originated from within the 160° to 190° wind sector, with wind speeds less than 3 ms^{-1}. Interestingly, a large benzene plume north of the HSC and the Battleground site was observed by a second TRACER-related project during the daytime of 23 September, reaching mixing ratios over 100 ppbv. While the two benzene peaks observed occurred at a different time and in a different location near the HSC, they highlight the spatial variability in VOC emissions across the industrial complex. Using a midpoint of the nighttime event observed in this study as the starting time for the NOAA dispersion model (01:30 a.m., 24 September), the estimated plume transport indicated a northbound path, reaching downwind communities such as Channelview, Highland, and Crosby within an hour (Figure 4). While the NOAA dispersion model can provide plume trajectories and dispersion patterns, including vertical resolution, the model's estimation is based on the

user-input plume release height, which may not represent the initial emission height and thereby the vertical extent of the plume. The estimated transport described here makes some assumptions about the event, such as only considering a single time point that may not represent the entire event period. Also, using the Battleground site as the start of the dispersion model assumes a single emission point for the plume and does not account for the spatial width of the plume influencing the Battleground site.

These nighttime emissions of benzene coincide with the potential formation of the primary nighttime oxidants, nitrate radicals (NO_3), which can be present in concentrations ranging from 50 to 500 pptv in Houston [35]. Combined with benzene's low nitrate reactivity ($k_{NO3} \approx <3 \times 10^{-17}$ cm^{-3} mol^{-1} s^{-1}), the benzene loss due to interactions with NO_3 is expected to be minimal and has been previously described by Qu et al. [36] and Huang et al. [37–40]. Alternatively, benzene has a larger reactivity with the daytime primary atmospheric oxidants, hydroxyl radicals (OH; $k_{OH} \approx 1.2 \times 10^{-12}$ cm^{-3} mol^{-1} s^{-1}), which are largely absent at night due to the lack of sunlight [39]. However, a recent study has shown that the formation of OH radicals can occur without light or heat in the presence of aqueous droplets, which represents a potential loss pathway at night [41]. Additionally, the lower nighttime boundary layer height may result in trapping the benzene near the surface and preventing vertical dispersion, allowing it to persist until photochemical reactions resume during daylight hours. Furthermore, slow, steady wind speeds at night may promote the retention of VOCs within the urban airshed, limiting vertical mixing and contributing to higher localized mixing ratios, compared to faster, erratic wind speeds that disperse the VOCs and reduce their local impact. Finally, benzene oxidation rates can be influenced by changes in relative humidity, as higher humidity levels can enhance certain oxidation pathways and lead to more efficient aqueous-phase chemistry.

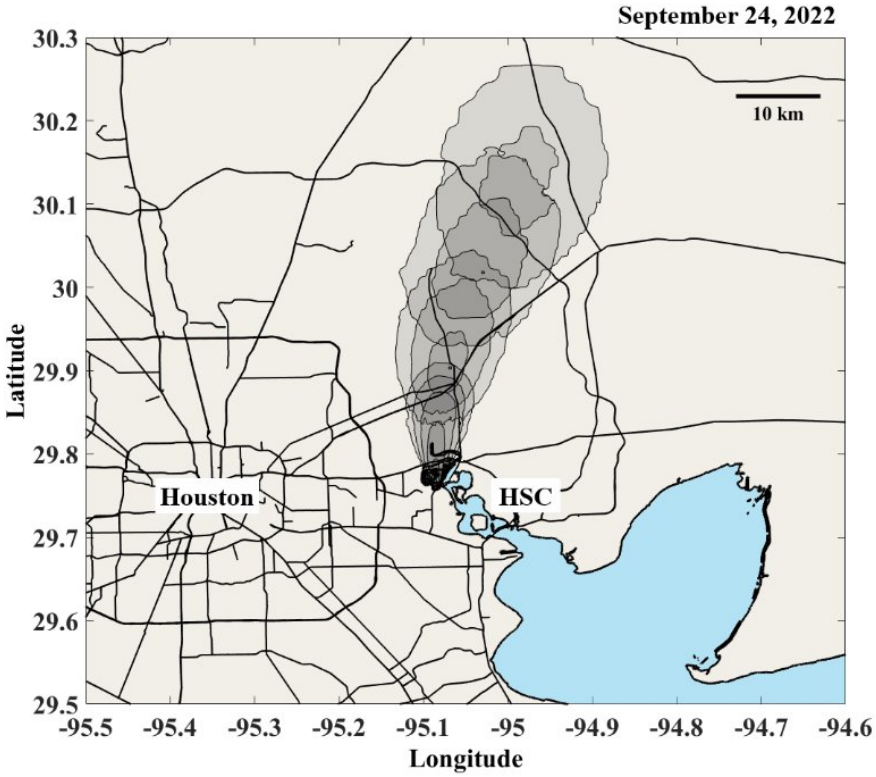

Figure 4. NOAA HYSPLIT dispersion model starting at the Battleground site for 1:30 on 24 September 2022. Each iterative plume represents the modeled transport within the last hour.

3.3. Acetone

Acetone was the most abundant VOC observed at the Battleground site during both TRACER campaigns. In this study, mixing ratios exceeding 150 ppbv, with routine peaks above 50 ppbv during both campaigns, were observed (Figure 1b). In contrast, ambient mixing ratios of acetone in urban areas typically range from 2 to 12 ppbv [42–45]. Acetone can be emitted from petrochemical activities such as burning and refining fossil fuels; however, acetone is used in several consumer applications, including solvent-based coatings, paint thinners, and architectural paints [46]. In addition, acetone can also be formed in the atmosphere through oxidation processes of biogenic (i.e., monoterpenes) and anthropogenic (i.e., alkanes) species, making it a frequently identified oxygenated VOC (OVOC) in urban emission inventories [47–52]. In particular, acetone has been shown to be a major product of propane atmospheric degradation, accounting for 80% of propane on a carbon basis [47,52]. Biogenic sources can also emit acetone as a by-product in plant metabolic processes, but they typically account for <20% of acetone mixing ratios; thus, they are considered a minor source [42,52,53]. Similar to benzene, atmospheric acetone is mainly removed by photolysis and reactions with OH radicals ($k_{OH} \approx 0.2 \times 10^{-12}$ cm^{-3} mol^{-1} s^{-1}), compared to the slower reaction rate with NO_3 radicals ($k_{NO3} \approx <3 \times 10^{-17}$ cm^{-3} mol^{-1} s^{-1}), resulting in an estimated lifetime of over eight years [39,49]. Additionally, acetone contributes to the formation of peroxy and alkoxy radicals, interacts with nitrogen oxides (NO_x), and participates in the formation of peroxyacetyl nitrate (PAN), which highlights acetone's role in tropospheric chemistry [54].

Acetone mixing ratios above 50 ppbv were measured on 7 unique nights in 2021 and 14 unique nights in 2022, accounting for 25 to 50% of the sampled days each month. These unique events ranged in duration from 2 to 4 h, with rates of changes reaching 15 ppbv per h, which suggests that biogenic emissions or atmospheric oxidation processes are most likely not responsible for such high levels of atmospheric acetone. In both years, the nighttime peaks originated from the same wind sectors, (mainly southwestern and western; Figure 2b,e), aligning with self-reported facilities in the emission inventory (Figure S3). Interestingly, daytime peaks in the acetone mixing ratios typically had durations lasting 8 to 10 h, increasing from 4 to 18 ppbv at a rate of approximately 3 ppbv per h. Acetone mixing ratios from 23 and 24 September 2021 highlight the differences between the acetone peaks associated with daytime and nighttime sources at the Battleground site (Figure 5). These time-series data suggest that the Battleground site was impacted by anthropogenic primary emission sources at night and correspond to daily fluctuations in jNO_2, aligning with secondary biogenic photooxidation sources during the daytime. The difference in peak shapes for acetone, including nighttime peaks with shorter durations and higher mixing ratios and daytime peaks exhibiting wider shapes and relatively lower concentrations compared to nighttime, highlights biogenic and photochemical oxidation of BVOCs as major sources during the daytime and intermittent industrial releases as a prominent source at nighttime. These peak mixing ratios represent a 7- to 30-fold increase over previous reports on urban traffic and secondary processing-related mixing ratios [43,44,54]. Similar to benzene, peaks in the acetone mixing ratios were relatively intermittent and were more consistently associated with nighttime activities as compared to daytime activities (Figure 1e). Self-reported industrial acetone sources in the HSC include activities such as thermal oxidation, coatings and painting in metal barrel and drum production, fugitive solvent leaks, and wastewater clarification.

Interestingly, sharp nighttime peaks were observed during both measurement campaigns (Figure 1b,e), with the daytime peaks being more pronounced in 2021 as compared to 2022. The year-to-year variability in daytime mixing ratios illustrated here highlights the complexity associated with characterizing OVOCs that can be either directly emitted into

the atmosphere as primary VOCs or formed indirectly from secondary processing. During both campaigns, acetone concentrations showed weak or no correlations with isoprene, other measured VOCs, and carbon monoxide (r^2 values < 0.06; Figures S10–S12). The only exception was for daytime acetone and benzene in 2022, with wind directions curtailed between 135 and 225°, which had an r^2 of 0.6 (Figure S13). The lack of relationships between acetone and other species suggests that acetone, benzene, and isoprene sources are likely not emitted from the same sources and rather could be related to a variety of densely co-located local industrial sources within the HSC.

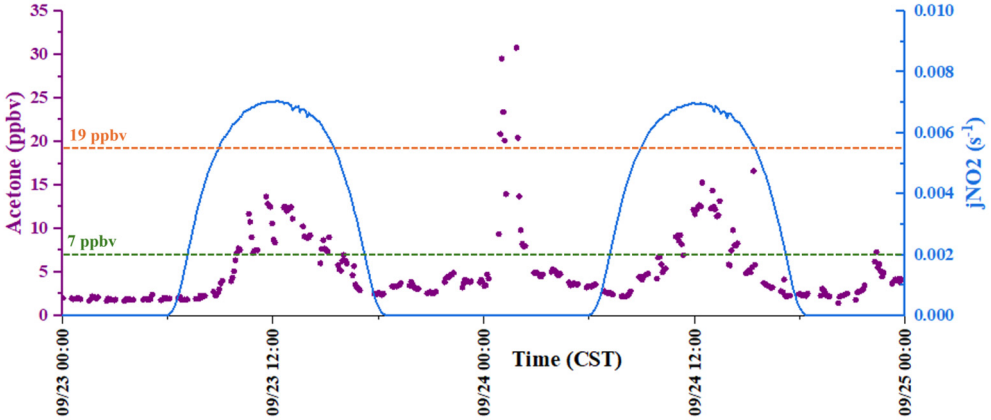

Figure 5. Time series of acetone mixing ratios (purple trace, 5 min-averaged) from 23 to 25 September 2021, with three peaks in acetone mixing ratios observed. The lower dashed line (green) represents the monthly average (μ = 7 ppbv), and the upper dashed line (orange) represents the monthly average and one standard deviation ($\mu + \sigma$ = 19 ppbv). The blue trace represents the average jNO_2 diurnal profile measured in September 2021.

The overlap of direct acetone emissions and secondary oxidation chemistry in a multifaceted emission environment complicates source attribution. This challenge is further exacerbated by the high source density within the HSC, which introduces spatial and temporal variability in the emission patterns that are difficult to resolve with the current source apportionment modeling capabilities. Furthermore, the reliance on facility-reported and yearly averaged emission data, rather than real-time or seasonal data, further impacts our ability to accurately model air quality impacts from specific activities and distinguish contributions from primary emissions and secondary formation processes.

3.4. Isoprene

Isoprene, a major component of global biogenic VOC emissions (1 Pg), plays a critical role in O_3 formation, especially in the presence of NO_x in urban areas [55]. Isoprene can be highly reactive with atmospheric oxidants ($k_{OH} \approx 100 \times 10^{-12}$ cm^{-3} mol^{-1} s^{-1}), leading to an atmospheric lifetime of only a few hours [39,56]. Biogenic emissions typically range from 1 to 4 ppbv and are emitted as a response to vegetative stress caused by solar radiation. Therefore, biogenic emissions are in part dependent on solar radiation and temperature, resulting in predictable diurnal and seasonal patterns [57,58]. Deviations from the typical biogenic-related diurnal profile, including temporal changes, magnitude increases, and rates of change, can provide an indication of changes in local sources and distinguish between biogenic and anthropogenic isoprene sources. In urban areas, biogenic isoprene often dominates emissions, while anthropogenic sources, such as traffic and human breath, contribute minimally, accounting for less than 10% of the total isoprene observed (1 ppbv) [59–61]. Isoprene is also produced and used in various industrial processes, including ethylene production and as a chemical feedstock (i.e., VCP component) [62,63].

These industrial sources can significantly impact urban air pollution near manufacturing facilities, but their emissions from such anthropogenic sources is limited. Most notably, isoprene recovered from ethylene production processes (e.g., naphtha cracking), can be used as a starting compound to form several products, including synthetic rubber for tires and block polymers (e.g., styrene–isoprene–styrene or SIS), or be converted into terpenes for VCP production [62–64]. Like other industrial-related VOC emissions, industrial isoprene emission profiles are likely more sporadic, as they are driven by the variability in industrial activities linked to product demand and operational conditions [19,26].

Typical urban isoprene mixing ratios range from 0.1 to 2.5 ppbv and are the combined impact of both biogenic and anthropogenic sources [57–60,65,66]. In this study, the daytime isoprene mixing ratio average in both years (1.3 ± 2.3 ppbv in 2021 and 1.3 ± 0.9 ppbv in 2022) fell within reported literature ranges (Figure 1c). The daytime profiles in both campaigns followed the ~12 h biogenic profile (i.e., <1 ppbv increase per h), with a peak from 12:00 to 14:00 along with solar radiation and then a decrease (<1 ppbv per h). However, similar to benzene and acetone, the September 2021 nighttime mixing ratios were observed to be above 30 ppbv on 10 unique sampling days (~30%) (Figure 1c,f). For example, on 18 September 2021, a peak mixing ratio above 110 ppbv was observed at 2:00, representing an over 35-fold increase compared to the average.

The nightly mixing ratio peaks represent a 10-fold increase over the daily average and typically lasted from 1 to 3 h and increased at rates of ~20 ppbv per h. These rapid changes in nighttime isoprene mixing ratios (peaking between 30 and 100 ppbv) suggest the presence of local nighttime emission sources and help to dismiss traditional biogenic daytime sources [19]. In the HSC, self-reported industrial isoprene sources include fugitive emissions from railcar loading, solvent storage tank flaring, and vapor recovery unit leaks. In an urban setting, isoprene is expected to have a relatively short nighttime atmospheric half-life (<1 h), as it readily reacts with NO_3 radicals [35,67]. However, periods of elevated nighttime mixing ratios of isoprene or other reactive VOCs may result in the rapid depletion of NO_3 radicals. Moreover, elevated mixing ratios of the reactive VOCs observed (total mixing ratios over 100 ppbv), including aromatics, alkanes, and oxygenated species, can influence NO_x chemistry and lead to a NO_x-limited regime, which has been observed previously in nighttime urban outflow in China's Pearl River Delta [68]. Furthermore, nighttime industrial VOC plumes can traverse the urban landscape and mix with urban traffic emissions, thereby potentially altering morning oxidation conditions in Houston, which are typically VOC-limited [19,69], and may subsequently influence O_3 formation downwind of the HSC.

In 2021, elevated periods of industrial isoprene emissions aligned with specific wind directions (90° to 135° and 190° to 225° sectors) and over 55 self-reported isoprene sources identified in the TCEQ point source emission inventory within 8 km of Battleground (Figure S4 in this study and Figure 7 in Shrestha et al. [19]). When compared to styrene, no direct correlation was observed, suggesting that polymer production may not have influenced the emissions (e.g., fugitive, cracking, or transport emissions; Figure S4). However, as both isoprene and styrene are involved in the production of SIS, their emissions may be associated with different production stages or specific activities. Interestingly, isoprene peaks occurred throughout the nighttime hours, while styrene peaks in mixing ratios were more focused near 6:00 to 9:00 and 17:00 to 19:00. It is important to note that other VOC fragments (e.g., peroxy isobutyryl nitrate; PiBN) may also contribute to m/z = 105 and interfere with styrene measurements by introducing sampling artifacts [70,71]. As suggested by de Gouw et al. [72], studies close to emission sources, such as petrochemical industries, are likely dominated by styrene measurements, and well-aged air masses are likely dominated by PiBN.

In contrast to TRACER 2021, the 2022 isoprene diurnal profile reflects a primarily biogenic influence, which highlights the year-to-year variability in the near-facility area (Figure 6). While industrial emission activities did not likely cease in this area in 2022, the type of activity may have changed, resulting in a temporal shift or reduction in isoprene emissions during September. Variability in facility activities can be driven by changes in consumer demand for the products they produce. Additionally, VCP production and use will vary with external factors, such as market fluctuations and feedstock availability, which may also impact industrial isoprene emissions. For example, changes in the production of styrene–isoprene–styrene (SIS) thermoplastic may impact the emissions and subsequent ambient mixing ratios of both styrene and isoprene. Interestingly, the diurnal mean profile for styrene in 2022 (as compared to 2021) showed a strong reduction in the early-morning and late-evening spikes (10+ ppbv; Figures S6f and S14). Additional external factors, such as policy changes and meteorological conditions, were not observed here but could impact the variability of industrial emissions in the future. Unlike the benzene and acetone peaks observed in both years, the isoprene reduction from 2021 to 2022 indicates the potential variability in the industrial emission composition, which would not be captured using a singular, consistent assumption of total emissions (i.e., annual emission inventory data). Oftentimes, the biogenic contributors to O_3 formation (i.e., isoprene and monoterpenes) are not considered for regulation because of their natural sources. However, as anthropogenic isoprene emissions are typically overlooked, they may be an important anthropogenic VOC for air quality managers to consider in the future, especially in areas downwind of large-scale industrial complexes. Furthermore, industrial isoprene emission factors may also be under-characterized and represent an important addition to the chemical modeling of the VCP supply chain.

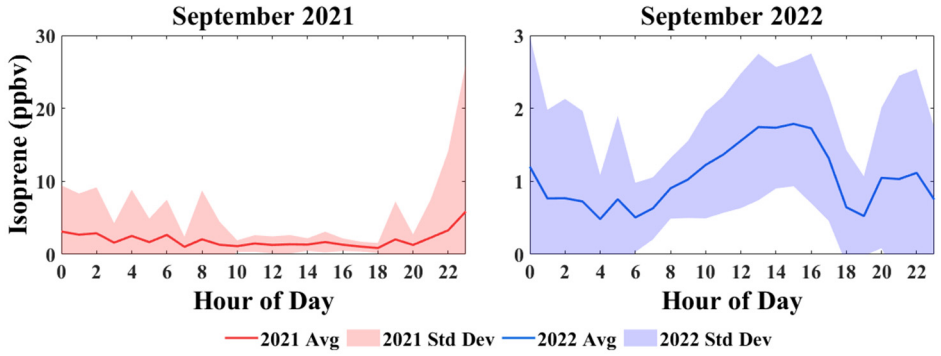

Figure 6. Diurnal mean profiles of isoprene measured in September 2021 (red trace) and September 2022 (blue trace) in the HSC with properly scaled axes. The shading represents the $\mu \pm \sigma$ of each dataset. Note: The y-axis for September 2021 is an order of magnitude larger than that for 2022.

4. Conclusions

This study utilized real-time VOC measurements at a site adjacent to the HSC during TRACER campaigns in September 2021 and 2022. The measurements captured the temporal variability in key VOCs, including benzene, toluene, acetone, styrene, and isoprene. For example, benzene, a HAP, consistently showed elevated nighttime mixing ratios (15+ ppbv) from a specific wind sector, suggesting local industrial sources as major contributors. These benzene observations support additional TRACER-related reports in the surrounding communities. Acetone, a key OVOC, displayed intermittent nighttime peaks, likely originating from a wide range of industrial activities. Additionally, acetone showed variability in daytime-related secondary formation between the two years, revealing a contribution from a mixture of sources within the industrial complex. Isoprene, traditionally associated with biogenic emissions, also presented nighttime peaks, indicating potential industrial

contributions. Wind direction and annual emission inventories also suggested local industrial sources of isoprene, while temporal data suggested that traffic and biogenic sources were not contributors to peak isoprene events. This analysis also highlights a shift in the relative contributions of biogenic VOC emissions from biogenic sources towards industrial emissions. Results from this study identify multiple VOCs with periods of elevated mixing ratios above 15 ppbv and often above 50 ppbv. Mixing ratios exceeding 15 ppbv were observed for at least one VOC on 58% of nights (n = 32 nights), with 19 nights (~35%) having two or more VOCs with mixing ratios above 15 ppbv. Subsequently, plume models of selected events highlight the possibility of VOC transport from areas in and around the industrial complex to the surrounding communities.

Identifying the specific sources and activities associated with these periods of elevated VOCs represents a significant knowledge gap in the current understanding of VOCs in areas like the HSC and the subsequent impacts on local communities. The high density of potential sources, combined with variability in the operational activities at each facility, makes source identification for a single compound during a single event extremely difficult. VOC emissions can occur across multiple chemical processing and handling steps, including loading and unloading, equipment leaks, tank cleaning, and chemical transfers. These challenges directly impact our ability to assess the relationship between various or specific industrial or chemical processing activities and VOC emissions. The specific processes and technology used (e.g., portable vapor combustion units) and the frequency of these activities will contribute to overall VOC emissions. Where local industrial emissions can dominate, VOCs such as isoprene, which is typically considered biogenic, may be considered anthropogenic. The overlap between industrial, traffic, biogenic, and secondary formation sources underscores the complexity of characterizing VOC emissions in industrial regions like the HSC.

To address these source identification challenges, more near-facility measurements are needed, as self-reported annual emission records are limited in their ability to characterize rapid changes in VOC emissions. Higher-resolution VOC emission data would be important for environmental policymakers and air quality managers as they work to improve air quality for downwind communities. For example, potential experiments may include more frequent and targeted measurements of VOCs released during specific industrial activities (i.e., chemical loading and unloading, transport, and storage) to help understand and address the short-term plume emissions observed in this study. Additionally, seasonal studies would further clarify the temporal resolution of industrial-related VOC emissions and expand on the self-reported annual emission values. Targeted nighttime mobile measurements guided by wind direction could also help map plume origins and transport within these dense industrial areas. This approach could involve either driving through the industrial complex at night or collaborating with individual companies to access industrial properties. These measurements would enable the capture of maximum and minimum VOC mixing ratios associated with nighttime industrial activities and assessment of the variability associated with specific activities. Finally, mobile air quality measurements in downwind communities could also provide community-level assessment opportunities to evaluate potential plume transport and mixing. The elevated VOC mixing ratios identified in this study may be of future interest and importance for understanding urban air quality near petrochemical industrial areas, particularly during periods of low wind or recirculation events. This would be especially important for downwind communities that are routinely impacted by motor vehicle exhaust and are typically VOC-sensitive with respect to air pollution and O_3 formation. Industrial isoprene emissions are of particular interest, as isoprene can support the formation of O_3 and SOA, which is dependent on the relative abundance of other air quality pollutants (e.g., NO_x) in downwind or surrounding

communities. Vertical VOC measurements can also help understand post-emission vertical mixing and processing in the atmosphere. Interestingly, many of the VOCs described in this study can also serve as chemical feedstocks utilized in manufacturing end-use products, blurring the distinction between VCPs and their raw components associated with petrochemical manufacturing. Future work should also consider characterizing when select VOCs transition to being classified as VCPs as their emissions move from petrochemical refinement processes to chemical feedstock and consumer product manufacturing.

Supplementary Materials: The following supporting information can be downloaded at: https://www.mdpi.com/article/10.3390/atmos16030260/s1, Figure S1: Diagram depicting the methodology used during the study, including sampling, chemical analysis, data interpretation and visualization; Text S1: Calibration, field-based limit of detection (FLOD) and uncertainty associated with PTR-MS data and concentration calculation [71–75]; Table S1: 5-minute averaged method detection limit (MDL) and data recovery of the compounds analyzed in September 2021 and September 2022; Table S2: Dynamic linear range of the compounds analyzed in September 2021 and September 2022; Table S3: Correlation coefficients (r^2) of benzene, toluene, and C_8 isomers for the 2021 measurement campaign; Table S4: Correlation coefficients (r^2) of benzene, toluene, and C_8 isomers for the 2022 measurement campaign; Table S5: Potential sources, range of urban mixing ratios, and OH· and NO_3· reactivity coefficients for benzene, acetone, and isoprene [19,20,24,25,27–31,42–52,56–62]; Figure S2: Maps of benzene sources adjacent to the Battleground sampling site (denoted by a yellow pin), including their emission magnitude in tons per year (TPY) (a) and emission type (b); Figure S3: Maps of acetone sources adjacent to the Battleground sampling site (denoted by a yellow pin), including their emission magnitude in tons per year (TPY) (a) and emission type (b); Figure S4: Maps of isoprene sources adjacent to the Battleground sampling site (denoted by a yellow pin), including their emission magnitude in tons per year (TPY) (a) and emission type (b); Figure S5: HYSPLIT dispersion model inputs parameters for pollutant releases at San Jacinto Battleground on 24 September 2022, and 18 September 2021; Figure S6: Timeseries and diurnal mean profiles (average $\pm$ 1 σ) of benzene, toluene, and xylenes measured in September 2021 (red trace) and September 2022 (blue trace) in the HSC; Figure S7: Diurnal mean profile (average $\pm$ 1 σ) of toluene measured in September 2021 (red trace) and September 2022 (blue trace) in the HSC; Figure S8: Measured VOCs vs wind direction for toluene, xylenes, and styrene in 2021 (A–C) and 2022 (D–F); Figure S9: NOAA HYSPLIT dispersion model for 00:00 to 8:00 CST with a release location at the Battleground site on 18 September 2021; Figure S10: 2021 correlations between acetone and other measured VOCs; Figure S11: 2022 correlations between acetone and other measured VOCs; Figure S12: Correlations plots of CO and select measured VOCs in both measurement campaigns; Figure S13: Benzene vs acetone correlations for mixing ratios measured in the 135°–225° wind sector for September 2021 and 2022, colored by time of day; Figure S14: Correlations plots of nighttime (20:00–5:00) isoprene and styrene in both measurement campaigns.

Author Contributions: Conceptualization and methodology, S.U.; formal analysis, M.G. and S.U.; investigation, S.S. and S.Y.; data curation, S.S. and M.M.; writing—original draft preparation, M.G. and S.U.; writing—review and editing, S.S., M.M., S.Y., M.T.S.R. and J.H.F.III; visualization, M.T.S.R.; supervision and project administration, S.U.; funding acquisition, S.U. and J.H.F.III. All authors have read and agreed to the published version of the manuscript.

Funding: The preparation of this manuscript was funded through a grant from the TCEQ (project numbers: 582-22-31913-020 and 582-21-22317-015). The content, findings, opinions, and conclusions are the work of the authors and do not necessarily represent the findings, opinions, and conclusions of the TCEQ.

Institutional Review Board Statement: Not applicable.

Informed Consent Statement: Not applicable.

Data Availability Statement: The data presented in this study will be available on request from the corresponding author.

Acknowledgments: The authors would like to thank Rebecca Sheesley for her helpful conversations and efforts on the TRACER-AQ campaigns. The authors would also like to thank Kimberly Sauceda for conducting the VOC measurements during TRACER-AQ2 in 2022.

Conflicts of Interest: The authors declare no conflicts of interest.

References

1. John, H.; Seinfeld, S.N.P. *Atmospheric Chemistry and Physics: From Air pollution to Climate Change*, 2nd ed.; John Wiley & Sons, Inc.: Hoboken, NJ, USA, 2006.
2. Criteria Air Pollutants. Available online: https://www.epa.gov/criteria-air-pollutants (accessed on 12 August 2024).
3. Mcdonald, B.C.; Gentner, D.R.; Goldstein, A.H.; Harley, R.A. Long-Term Trends in Motor Vehicle Emissions in U.S. Urban Areas. *Environ. Sci. Technol.* **2013**, *47*, 10022–10031. [CrossRef] [PubMed]
4. McDonald, B.C.; de Gouw, J.A.; Gilman, J.B.; Jathar, S.H.; Akherati, A.; Cappa, C.D.; Jimenez, J.L.; Lee-Taylor, J.; Hayes, P.L.; McKeen, S.A.; et al. Volatile chemical products emerging as largest petrochemical source of urban organic emissions. *Science* **2018**, *359*, 760. [CrossRef] [PubMed]
5. Shah, R.U.; Coggon, M.M.; Gkatzelis, G.I.; Mcdonald, B.C.; Tasoglou, A.; Huber, H.; Gilman, J.; Warneke, C.; Robinson, A.L.; Presto, A.A. Urban Oxidation Flow Reactor Measurements Reveal Significant Secondary Organic Aerosol Contributions from Volatile Emissions of Emerging Importance. *Environ. Sci. Technol.* **2020**, *54*, 714–725. [CrossRef]
6. Coggon, M.M.; Gkatzelis, G.I.; Mcdonald, B.C.; Gilman, J.B.; Schwantes, R.H.; Abuhassan, N.; Aikin, K.C.; Arend, M.F.; Berkoff, T.A.; Brown, S.S.; et al. Volatile chemical product emissions enhance ozone and modulate urban chemistry. *Proc. Natl. Acad. Sci. USA* **2021**, *118*, e2026653118. [CrossRef] [PubMed]
7. Gkatzelis, G.I.; Coggon, M.M.; Mcdonald, B.C.; Peischl, J.; Gilman, J.B.; Aikin, K.C.; Robinson, M.A.; Canonaco, F.; Prevot, A.S.H.; Trainer, M.; et al. Observations Confirm that Volatile Chemical Products Are a Major Source of Petrochemical Emissions in U.S. Cities. *Environ. Sci. Technol.* **2021**, *55*, 4332–4343. [CrossRef] [PubMed]
8. Nault, B.A.; Jo, D.S.; Mcdonald, B.C.; Campuzano-Jost, P.; Day, D.A.; Hu, W.; Schroder, J.C.; Allan, J.; Blake, D.R.; Canagaratna, M.R.; et al. Secondary organic aerosols from anthropogenic volatile organic compounds contribute substantially to air pollution mortality. *Atmos. Chem. Phys.* **2021**, *21*, 11201–11224. [CrossRef]
9. Clews, R.J. Chapter 5—Fundamentals of the Petroleum Industry. In *Project Finance for the International Petroleum Industry*; Clews, R.J., Ed.; Academic Press: San Diego, CA, USA, 2016; pp. 83–99.
10. Barrett, K. More Counties Saw Population Gains in 2023. Available online: https://www.census.gov/newsroom/press-releases/2024/population-estimates-more-counties-population-gains-2023.html (accessed on 19 September 2024).
11. Ryerson, T.B. Effect of petrochemical industrial emissions of reactive alkenes and NOxon tropospheric ozone formation in Houston, Texas. *J. Geophys. Res.* **2003**, *108*, 4249. [CrossRef]
12. Jobson, B.T.; Berkowitz, C.M.; Kuster, W.C.; Goldan, P.D.; Williams, E.J.; Fesenfeld, F.C.; Apel, E.C.; Karl, T.; Lonneman, W.A.; Riemer, D. Hydrocarbon source signatures in Houston, Texas: Influence of the petrochemical industry. *J. Geophys. Res. Atmos.* **2004**, *109*, D24305. [CrossRef]
13. Kleinman, L.I.; Daum, P.H.; Imre, D.; Lee, Y.-N.; Nunnermacker, L.J.; Springston, S.R.; Weinstein-Lloyd, J.; Rudolph, J. Ozone production rate and hydrocarbon reactivity in 5 urban areas: A cause of high ozone concentration in Houston. *Geophys. Res. Lett.* **2002**, *29*, 105-1–105-4. [CrossRef]
14. Kleinman, L.I.; Daum, P.H.; Lee, Y.-N.; Nunnermacker, L.J.; Springston, S.R.; Weinstein-Lloyd, J.; Rudolph, J. A comparative study of ozone production in five U.S. metropolitan areas. *J. Geophys. Res. Atmos.* **2005**, *110*, D02301. [CrossRef]
15. Parrish, D.D.; Allen, D.T.; Bates, T.S.; Estes, M.; Fehsenfeld, F.C.; Feingold, G.; Ferrare, R.; Hardesty, R.M.; Meagher, J.F.; Nielsen-Gammon, J.W.; et al. Overview of the Second Texas Air Quality Study (TexAQS II) and the Gulf of Mexico Atmospheric Composition and Climate Study (GoMACCS). *J. Geophys. Res. Atmos.* **2009**, *114*, D00F13. [CrossRef]
16. Pierce, R.B.; Al-Saadi, J.; Kittaka, C.; Schaack, T.; Lenzen, A.; Bowman, K.; Szykman, J.; Soja, A.; Ryerson, T.; Thompson, A.M.; et al. Impacts of background ozone production on Houston and Dallas, Texas, air quality during the Second Texas Air Quality Study field mission. *J. Geophys. Res. Atmos.* **2009**, *114*, D00F09. [CrossRef]
17. Gilman, J.B.; Kuster, W.C.; Goldan, P.D.; Herndon, S.C.; Zahniser, M.S.; Tucker, S.C.; Brewer, W.A.; Lerner, B.M.; Williams, E.J.; Harley, R.A.; et al. Measurements of volatile organic compounds during the 2006 TexAQS/GoMACCS campaign: Industrial influences, regional characteristics, and diurnal dependencies of the OH reactivity. *J. Geophys. Res. Atmos.* **2009**, *114*, D00F06. [CrossRef]

18. Mazzuca, G.M.; Ren, X.; Loughner, C.P.; Estes, M.; Crawford, J.H.; Pickering, K.E.; Weinheimer, A.J.; Dickerson, R.R. Ozone production and its sensitivity to NOx and VOCs: Results from the DISCOVER-AQ field experiment, Houston 2013. *Atmos. Chem. Phys.* **2016**, *16*, 14463–14474. [CrossRef]
19. Shrestha, S.; Yoon, S.; Alvarez, S.L.; Wang, Y.; Flynn, J.H.; Usenko, S.; Sheesley, R.J. Emission Ratios and Diurnal Variability of Volatile Organic Compounds and Influence of Industrial Emissions in Two Texas Cities. *Atmosphere* **2023**, *14*, 1006. [CrossRef]
20. Shrestha, S.; Yoon, S.; Erickson, M.H.; Guo, F.; Mehra, M.; Bui, A.A.T.; Schulze, B.C.; Kotsakis, A.; Daube, C.; Herndon, S.C.; et al. Traffic, transport, and vegetation drive VOC concentrations in a major urban area in Texas. *Sci. Total Environ.* **2022**, *838*, 155861. [CrossRef]
21. Jobson, B.T.; McCoskey, J.K. Sample drying to improve HCHO measurements by PTR-MS instruments: Laboratory and field measurements. *Atmos. Chem. Phys.* **2010**, *10*, 1821–1835. [CrossRef]
22. Mehra, M.; Shrestha, S.; Ap, K.; Guagenti, M.; Moffett, C.E.; VerPloeg, S.G.; Coogan, M.A.; Rai, M.; Kumar, R.; Andrews, E.; et al. Atmospheric heating in the US from saharan dust: Tracking the June 2020 event with surface and satellite observations. *Atmos. Environ.* **2023**, *310*, 119988. [CrossRef]
23. Robinson, E.S.; Tehrani, M.W.; Yassine, A.; Agarwal, S.; Nault, B.A.; Gigot, C.; Chiger, A.A.; Lupolt, S.N.; Daube, C.; Avery, A.M.; et al. Ethylene Oxide in Southeastern Louisiana's Petrochemical Corridor: High Spatial Resolution Mobile Monitoring during HAP-MAP. *Environ. Sci. Technol.* **2024**, *58*, 11084–11095. [CrossRef] [PubMed]
24. Buczynska, A.J.; Krata, A.; Stranger, M.; Locateli Godoi, A.F.; Kontozova-Deutsch, V.; Bencs, L.; Naveau, I.; Roekens, E.; Van Grieken, R. Atmospheric BTEX-concentrations in an area with intensive street traffic. *Atmos. Environ.* **2009**, *43*, 311–318. [CrossRef]
25. Cao, C.; Gentner, D.R.; Commane, R.; Toledo-Crow, R.; Schiferl, L.D.; Mak, J.E. Policy-Related Gains in Urban Air Quality May Be Offset by Increased Emissions in a Warming Climate. *Environ. Sci. Technol.* **2023**, *57*, 9683–9692. [CrossRef] [PubMed]
26. Sadeghi, B.; Pouyaei, A.; Choi, Y.; Rappenglueck, B. Influence of seasonal variability on source characteristics of VOCs at Houston industrial area. *Atmos. Environ.* **2022**, *277*, 119077. [CrossRef]
27. Jephcote, C.; Mah, A. Regional inequalities in benzene exposures across the European petrochemical industry: A Bayesian multilevel modelling approach. *Environ. Int.* **2019**, *132*, 104812. [CrossRef] [PubMed]
28. Miller, D.; Armstrong, K.; Styring, P. Assessing methods for the production of renewable benzene. *Sustain. Prod. Consum.* **2022**, *32*, 184–197. [CrossRef]
29. Vaughan, B.A.; Webster-Gardiner, M.S.; Cundari, T.R.; Gunnoe, T.B. A rhodium catalyst for single-step styrene production from benzene and ethylene. *Science* **2015**, *348*, 421–424. [CrossRef]
30. Meng, Q.; Yan, J.; Wu, R.; Liu, H.; Sun, Y.; Wu, N.; Xiang, J.; Zheng, L.; Zhang, J.; Han, B. Sustainable production of benzene from lignin. *Nat. Commun.* **2021**, *12*, 4534. [CrossRef]
31. Deloitte. *The Future of Petrochemicals: Growth Surrounded by Uncertainty*; Deloitte Development LLC: London, UK, 2019.
32. Strott, S. Levels of Cancer-Causing Benzene Reached New Heights in Beleaguered Channelview, Texas. Regulators Never Told Residents. *Public Health Watch*, 12 December 2024.
33. Dantas, G.; Gorne, I.; da Silva, C.M.; Arbilla, G. Benzene, Toluene, Ethylbenzene and Xylene (BTEX) Concentrations in Urban Areas Impacted by Chemical and Petrochemical Industrial Emissions. *Bull. Environ. Contam. Toxicol.* **2022**, *108*, 204–211. [CrossRef]
34. Cui, L.; Wu, D.; Wang, S.; Xu, Q.; Hu, R.; Hao, J. Measurement report: Ambient volatile organic compound (VOC) pollution in urban Beijing: Characteristics, sources, and implications for pollution control. *Atmos. Chem. Phys.* **2022**, *22*, 11931–11944. [CrossRef]
35. Stutz, J.; Wong, K.W.; Lawrence, L.; Ziemba, L.; Flynn, J.H.; Rappenglück, B.; Lefer, B. Nocturnal NO_3 radical chemistry in Houston, TX. *Atmos. Environ.* **2010**, *44*, 4099–4106. [CrossRef]
36. Qu, X.; Zhang, Q.; Wang, W. Degradation mechanism of benzene by NO_3 radicals in the atmosphere: A DFT study. *Chem. Phys. Lett.* **2006**, *426*, 13–19. [CrossRef]
37. Atkinson, R.; Plum, C.N.; Carter, W.P.L.; Winer, A.M.; Pitts, J.N. Rate Constants for the Gas-Phase Reactions of Nitrate Radicals with a Series of Organics in Air at 298 +/− 1-K. *J. Phys. Chem.* **1984**, *88*, 1210–1215. [CrossRef]
38. Atkinson, R.; Baulch, D.L.; Cox, R.A.; Hampson, R.F.; Kerr, J.A.; Rossi, M.J.; Troe, J. Evaluated kinetic and photochemical data for atmospheric chemistry, organic species: Supplement VII. *J. Phys. Chem. Ref. Data* **1999**, *28*, 191–393. [CrossRef]
39. Atkinson, R.; Arey, J. Atmospheric Degradation of Volatile Organic Compounds. *Chem. Rev.* **2003**, *103*, 4605–4638. [CrossRef] [PubMed]
40. Huang, M.; Liao, Y.; Wang, Z.; Hao, L.; Zhang, W. A theoretical investigation of NO_3-initiated oxidation of toluene. *Comput. Theor. Chem.* **2014**, *1037*, 63–69. [CrossRef]
41. Li, K.; Guo, Y.; Nizkorodov, S.A.; Rudich, Y.; Angelaki, M.; Wang, X.; An, T.; Perrier, S.; George, C. Spontaneous dark formation of OH radicals at the interface of aqueous atmospheric droplets. *Proc. Natl. Acad. Sci. USA* **2023**, *120*, e2220228120. [CrossRef] [PubMed]

42. Hu, L.; Millet, D.B.; Kim, S.Y.; Wells, K.C.; Griffis, T.J.; Fischer, E.V.; Helmig, D.; Hueber, J.; Curtis, A.J. North American acetone sources determined from tall tower measurements and inverse modeling. *Atmos. Chem. Phys.* **2013**, *13*, 3379–3392. [CrossRef] [PubMed]
43. de Gouw, J.A.; Gilman, J.B.; Kim, S.-W.; Alvarez, S.L.; Dusanter, S.; Graus, M.; Griffith, S.M.; Isaacman-VanWertz, G.; Kuster, W.C.; Lefer, B.L.; et al. Chemistry of Volatile Organic Compounds in the Los Angeles Basin: Formation of Oxygenated Compounds and Determination of Emission Ratios. *J. Geophys. Res. Atmos.* **2018**, *123*, 2298–2319. [CrossRef]
44. Wu, C.; Wang, C.; Wang, S.; Wang, W.; Yuan, B.; Qi, J.; Wang, B.; Wang, H.; Wang, C.; Song, W.; et al. Measurement report: Important contributions of oxygenated compounds to emissions and chemistry of volatile organic compounds in urban air. *Atmos. Chem. Phys.* **2020**, *20*, 14769–14785. [CrossRef]
45. Liu, X.F.; Li, X.Y.; Tan, X.; Bai, H.L.; Li, Y.Y.; Zhang, S.T. Distribution characteristics, source apportionment, and chemical reactivity of volatile organic compounds in two adjacent areas in Shanxi, North China. *Atmos. Environ.* **2022**, *290*, 119374. [CrossRef]
46. Seltzer, K.M.; Pennington, E.; Rao, V.; Murphy, B.N.; Strum, M.; Isaacs, K.K.; Pye, H.O.T. Reactive organic carbon emissions from volatile chemical products. *Atmos. Chem. Phys.* **2021**, *21*, 5079–5100. [CrossRef]
47. Rosado-Reyes, C.M.; Francisco, J.S. Atmospheric oxidation pathways of propane and its by-products: Acetone, acetaldehyde, and propionaldehyde. *J. Geophys. Res. Atmos.* **2007**, *112*, D14310. [CrossRef]
48. Vereecken, L.; Peeters, J. Theoretical Study of the Formation of Acetone in the OH-Initiated Atmospheric Oxidation of α-Pinene. *J. Phys. Chem. A* **2000**, *104*, 11140–11146. [CrossRef]
49. Reissell, A.; Harry, C.; Aschmann, S.M.; Atkinson, R.; Arey, J. Formation of acetone from the OH radical- and O_3-initiated reactions of a series of monoterpenes. *J. Geophys. Res. Atmos.* **1999**, *104*, 13869–13879. [CrossRef]
50. Jacob, D.J.; Field, B.D.; Jin, E.M.; Bey, I.; Li, Q.; Logan, J.A.; Yantosca, R.M.; Singh, H.B. Atmospheric budget of acetone. *J. Geophys. Res. Atmos.* **2002**, *107*, ACH 5-1–ACH 5-17. [CrossRef]
51. Goldstein, A.H.; Schade, G.W. Quantifying biogenic and anthropogenic contributions to acetone mixing ratios in a rural environment. *Atmos. Environ.* **2000**, *34*, 4997–5006. [CrossRef]
52. Singh, H.B.; O'Hara, D.; Herlth, D.; Sachse, W.; Blake, D.R.; Bradshaw, J.D.; Kanakidou, M.; Crutzen, P.J. Acetone in the atmosphere: Distribution, sources, and sinks. *J. Geophys. Res. Atmos.* **1994**, *99*, 1805–1819. [CrossRef]
53. Jardine, K.J.; Sommer, E.D.; Saleska, S.R.; Huxman, T.E.; Harley, P.C.; Abrell, L. Gas Phase Measurements of Pyruvic Acid and Its Volatile Metabolites. *Environ. Sci. Technol.* **2010**, *44*, 2454–2460. [CrossRef] [PubMed]
54. Guo, H.; Ling, Z.H.; Cheung, K.; Wang, D.W.; Simpson, I.J.; Blake, D.R. Acetone in the atmosphere of Hong Kong: Abundance, sources and photochemical precursors. *Atmos. Environ.* **2013**, *65*, 80–88. [CrossRef]
55. Guenther, A.B.; Jiang, X.; Heald, C.L.; Sakulyanontvittaya, T.; Duhl, T.; Emmons, L.K.; Wang, X. The Model of Emissions of Gases and Aerosols from Nature version 2.1 (MEGAN2.1): An extended and updated framework for modeling biogenic emissions. *Geosci. Model Dev.* **2012**, *5*, 1471–1492. [CrossRef]
56. Bates, K.H.; Jacob, D.J. A new model mechanism for atmospheric oxidation of isoprene: Global effects on oxidants, nitrogen oxides, organic products, and secondary organic aerosol. *Atmos. Chem. Phys.* **2019**, *19*, 9613–9640. [CrossRef]
57. Park, C.; Schade, G.W.; Boedeker, I. Characteristics of the flux of isoprene and its oxidation products in an urban area. *J. Geophys. Res. Atmos.* **2011**, *116*, D21303. [CrossRef]
58. Bryant, D.J.; Nelson, B.S.; Swift, S.J.; Budisulistiorini, S.H.; Drysdale, W.S.; Vaughan, A.R.; Newland, M.J.; Hopkins, J.R.; Cash, J.M.; Langford, B.; et al. Biogenic and anthropogenic sources of isoprene and monoterpenes and their secondary organic aerosol in Delhi, India. *Atmos. Chem. Phys.* **2023**, *23*, 61–83. [CrossRef]
59. Wagner, P.; Kuttler, W. Biogenic and anthropogenic isoprene in the near-surface urban atmosphere—A case study in Essen, Germany. *Sci. Total Environ.* **2014**, *475*, 104–115. [CrossRef]
60. Khan, M.A.H.; Schlich, B.-L.; Jenkin, M.E.; Shallcross, B.M.A.; Moseley, K.; Walker, C.; Morris, W.C.; Derwent, R.G.; Percival, C.J.; Shallcross, D.E. A Two-Decade Anthropogenic and Biogenic Isoprene Emissions Study in a London Urban Background and a London Urban Traffic Site. *Atmosphere* **2018**, *9*, 387. [CrossRef]
61. von Schneidemesser, E.; Monks, P.S.; Gros, V.; Gauduin, J.; Sanchez, O. How important is biogenic isoprene in an urban environment? A study in London and Paris. *Geophys. Res. Lett.* **2011**, *38*, L19804. [CrossRef]
62. Bertazzi, P.A.; Coggon, D.; Dragani, T.A.; Elwell, M.R.; Evans, H.J.; Filser, J.G.; Gerin, M.; Hemminki, K.; Hogstedt, C.; Kirsch-Volders, M.; et al. *IARC Monographs on the Evaluation of Carcinogenic Risks to Humans. Some Industrial Chemicals*; International Agency for Research on Cancer: Lyon, France, 1994.
63. Kothandaraman, J.; Cosimbescu, L.; Swita, M.S. Solvent-Induced Selectivity of Isoprene from Bio-Derived Prenol. *Front. Chem.* **2022**, *10*, 879129. [CrossRef]
64. Ezinkwo, G.O.; Tretjakov, V.F.; Talyshinky, R.M.; Ilolov, A.M.; Mutombo, T.A. Overview of the Catalytic Production of Isoprene from different raw materials; Prospects of Isoprene production from bio-ethanol. *Catal. Sustain. Energy* **2013**, *1*, 100–111. [CrossRef]
65. Li, G.; Zhang, R.; Fan, J.; Tie, X. Impacts of biogenic emissions on photochemical ozone production in Houston, Texas. *J. Geophys. Res. Atmos.* **2007**, *112*, D10309. [CrossRef]

66. Hu, L.; Millet, D.B.; Baasandorj, M.; Griffis, T.J.; Turner, P.; Helmig, D.; Curtis, A.J.; Hueber, J. Isoprene emissions and impacts over an ecological transition region in the U.S. Upper Midwest inferred from tall tower measurements. *J. Geophys. Res. Atmos.* **2015**, *120*, 3553–3571. [CrossRef]
67. Carter, W.; Atkinson, R. Development and Evaluation of a Detailed Mechanism for the Atmospheric Reactions of Isoprene and NO. *Int. J. Chem. Kinet.* **1996**, *28*, 497–530. [CrossRef]
68. Wang, J.; Wang, H.; Tham, Y.J.; Ming, L.; Zheng, Z.; Fang, G.; Sun, C.; Ling, Z.; Zhao, J.; Fan, S. Measurement report: Atmospheric nitrate radical chemistry in the South China Sea influenced by the urban outflow of the Pearl River Delta. *Atmos. Chem. Phys.* **2024**, *24*, 977–992. [CrossRef]
69. Ren, X.; van Duin, D.; Cazorla, M.; Chen, S.; Mao, J.; Zhang, L.; Brune, W.H.; Flynn, J.H.; Grossberg, N.; Lefer, B.L.; et al. Atmospheric oxidation chemistry and ozone production: Results from SHARP 2009 in Houston, Texas. *J. Geophys. Res. Atmos.* **2013**, *118*, 5770–5780. [CrossRef]
70. Kuster, W.C.; Jobson, B.T.; Karl, T.; Riemer, D.; Apel, E.; Goldan, P.D.; Fehsenfeld, F.C. Intercomparison of Volatile Organic Carbon Measurement Techniques and Data at La Porte during the TexAQS2000 Air Quality Study. *Environ. Sci. Technol.* **2004**, *38*, 221–228. [CrossRef] [PubMed]
71. de Gouw, J.A.; Goldan, P.D.; Warneke, C.; Kuster, W.C.; Roberts, J.M.; Marchewka, M.; Bertman, S.B.; Pszenny, A.A.P.; Keene, W.C. Validation of proton transfer reaction-mass spectrometry (PTR-MS) measurements of gas-phase organic compounds in the atmosphere during the New England Air Quality Study (NEAQS) in 2002. *J. Geophys. Res. Atmos.* **2003**, *108*, 4682. [CrossRef]
72. de Gouw, J.; Warneke, C. Measurements of volatile organic compounds in the earth's atmosphere using proton-transfer-reaction mass spectrometry. *Mass Spectrom. Rev.* **2007**, *26*, 223–257. [CrossRef] [PubMed]
73. Warneke, C.; de Gouw, J.A.; Kuster, W.C.; Goldan, P.D.; Fall, R. Validation of Atmospheric VOC Measurements by Proton-Transfer-Reaction Mass Spectrometry Using a Gas-Chromatographic Preseparation Method. *Environ. Sci. Technol.* **2003**, *37*, 2494–2501. [CrossRef] [PubMed]
74. de Gouw, J.; Warneke, C.; Karl, T.; Eerdekens, G.; van der Veen, C.; Fall, R. Sensitivity and specificity of atmospheric trace gas detection by proton-transfer-reaction mass spectrometry. *Int. J. Mass Spectrom.* **2003**, *223–224*, 365–382. [CrossRef]
75. Sinha, V.; Kumar, V.; Sarkar, C. Chemical composition of pre-monsoon air in the Indo-Gangetic Plain measured using a new air quality facility and PTR-MS: High surface ozone and strong influence of biomass burning. *Atmos. Chem. Phys.* **2014**, *14*, 5921–5941. [CrossRef]

Disclaimer/Publisher's Note: The statements, opinions and data contained in all publications are solely those of the individual author(s) and contributor(s) and not of MDPI and/or the editor(s). MDPI and/or the editor(s) disclaim responsibility for any injury to people or property resulting from any ideas, methods, instructions or products referred to in the content.